Hindawi
Advances in Civil Engineering
Volume 2022, Article ID 1797811, 12 pages
https://doi.org/10.1155/2022/1797811

Research Article

The Prediction of Cracking Load and Peak Load of UHPC-NC Composite Structure

Yanru Chen [1] **and Wei Mao** [2]

[1]*School of Civil and Environmental Engineering, Chengdu Jincheng Colleague, Chengdu 611731, China*
[2]*Southwest Municipal Engineering Design & Research Institute of China, Chengdu 610213, China*

Correspondence should be addressed to Yanru Chen; chenyanru@cdjcc.edu.cn

Received 6 September 2022; Revised 16 September 2022; Accepted 19 October 2022; Published 1 November 2022

Academic Editor: Claudio Mazzotti

In this study, models for calculating the cracking load and a peak load of the UHPC-NC structures are established. The effects of UHPC's high tensile strength, reinforced steel bars in NC, reinforce steel bars in UHPC, and prestress tendons in UHPC on cracking load and peak load are considered. In the cracking load model, UHPC is considered to be elastic and the stress distribution is triangular, the stress of steel bars and prestressing tendons is also calculated according to the plane section assumption and elastic theory. In the peak load module, UHPC is assumed to be partially elastic and partially plastic. The plastic part is represented by a rectangular stress block diagram, and the stress value reduction factor and rectangular stress frame height reduction factor are obtained by trial calculation. Compared with the experimental data of UHPC-NC beams with different types of combinations collected from references, the calculated results have a high matching degree, which is suitable for various types of UHPC-NC, both cracking loads and peak loads.

1. Introduction

Ultra-high-performance concrete (UHPC) is a new construction material developed by Richard and Cheyrezy in 1995 [1]. UHPC has been widely used in protecting structures and giant structures with slim designs. The UHPC has excellent mechanical properties, which include high strength in compression and tension [2–4], strain hardening [5] low permeability [3], high energy absorption, and durability [6]. Due to its superior performance, many researchers have studied the structural response of UHPC structures. Compared with the traditional reinforced concrete (RC) elements, the overall performance of the UHPC structure, including ultimate strength, stiffness, ductility behavior, and strain hardening, has been significantly improved. And it can effectively control crack width and ductility [7, 8].

UHPC also has excellent impact resistance and energy-absorbing capacity. Wei Fan et.al examined impact performances of UHPC columns by using the drop-hammer the impact test system, the results show the crashworthiness of the axially-loaded UHPC column was confirmed to be considerably superior to that of the conventional RC column [9]. Doo-Yeol Yoo et al. investigated the impact and blast resistances of UHPC and found that UHPC can dissipate much higher energy by impact than ordinary concrete [10]. To analyze the low-speed impact resistance of UHPC, Wei Guo et al. established the modified CSCM model, which was used to calculate the low-speed impact resistance of UHPC, and it was in good agreement with the experimental results [11]. Based on excellent properties, UHPC is used in structures that need to resist impact loads. It is used to strengthen traditional concrete columns. Three reinforcement forms have been completed by Wei Fan et.al, strengthened columns with two-end UHPC jackets are the better strengthening method [9]. The reinforcement method is used to improve the crashworthiness of bridge piers, and the impact of various parameters on the crashworthiness of bridge piers is analyzed by the response surface model [12, 13]. The combination of UHPC and steel structure has also been proven to have good impact resistance. Different types of core structures were experimentally investigated by scholars, and various models are simulated by the finite

element method, which proves that UHPC panels can effectively protect the structure under high energy impact [14].

UHPC is often used in repairing RC structures to improve the bearing capacity and resistance to impact load. of structures [9, 14–16]; it also is used combined with RC to improve the performance of RC structures and reduce the price of the UHPC structure [17, 18].

According to Mohammed and Isa, no matter whether sandblast the surfaces of the concrete beams and then cast UHPC around it inside a mold or bond prefabricated UHPC strips to the reinforced concrete beams using epoxy adhesive, the UHPC and normal concrete (NC) can work together, and the deformation accords with the assumption of plane section [18]. Sun and Liu have done experiments on strengthening reinforced concrete beams with the HSH-UHPC layer. The deflection, strain distribution, crack propagation, and failure mode are described in detail. The tests verified that the middle section of the UHPC-NC composite beam conforms to the assumption of the plane section [19].

Tatarstan et al. have done experiments to compare epoxy resin and mechanical anchorages of the UHPC layer on the *e* original RC beam [20]. Results show two methods can improve the peak load of the structure, the combination of the UHPC precast layer and reinforced concrete is good. Hussein and Amleh have done specimens using UHPC in tension and a normal strength concrete layer in compression. The result has shown that the proposed composite system was successfully enhanced in both flexural and shears capacity [21].

Many experimental studies have been done on the combination forms of UHPC-NC composite members. A detailed investigation of RC strengthened with UHPC at the bottom edge, top edge, and jacket was presented by Lampropoulos et al. [15]. The bottom edge, two longitudinal, and three sides reinforce the experimental and analytical investigation presented by Al-Osta et al. Experimental results show that the beams are strengthened on three sides with the highest capacity enhancement [18].

Safdar and Muhammad experimented with adding steel reinforcing bars in the added UHPC layer. By adding the UHPC layer on the tensile side, the stiffness can be greatly improved, the formation of cracks was delayed, and the peak load was slightly increased [22]. The experimental results of reference [13] show that the flexural resistance of UHPC-NC can be greatly improved by installing proper longitudinal reinforcement in the UHPC layer [19].

2. Materials and Methods

2.1. Specimen Test Collection and Classification. This paper collects some experimental samples of the UHPC-NC composite structure. Seven slab specimens were tested by AI-Osta et al. The UHPC strength RC beams from the bottom edge, longitudinal sides, and jacket, respectively [18]. Lampropoulos and Paschalis also conducted experiments with the top, bottom edge, and jacket, respectively [15].

Yin Hor et al. have tested two types of specimens. The first tested UHPC as a patch material for repairing deteriorated concrete structures; the second tested the UHPC as an overlay series used to retrofit soffits of RC beams [23]. Paschalis and Lampropoulos have tested full-scale RC beams strengthened with UHPC layers. Additional UHPU layers with and without steel reinforcing bars have been tested [24]. Safdar and Matsumoto have strengthened the RC beam in tension and compression zones, with UHPC of varying thicknesses [22]. LI wang–wang et al. have tested seven I-beams composed of UHPC and NC, and also considered the influence of varying steel reinforcing bars and prestressed reinforcement [25].

2.2. Material Properties of Specimens. Typically, the compressive strength of UHPC is much greater than that of normal concrete. All of the compressive strengths of UHPC in this paper exceeded 100 MPa, as shown in Figure 1; the tensile strength of UHPC is 11 MPa-18 MPa, as shown in Figure 2; the compressive strength of normal concrete is 30 MPa–60 MPa, as shown in Figure 3; and the strength of ordinary steel bars is 500 MPa–600 MPa. LI wang–wang's samples are added with high-strength prestress tendons in UHPC, and the design value of tensile strength is 1860 MPa [15, 18, 22–26].

All the samples consider the damage of UHPC in the tension zone; some use two-stage stress-strain curves, and some use multistage curves, as shown in Figure 4. Generally, the mechanical calculation model uses a two-stage formula, while the finite element model uses a two-stage or multistage formula.

The two-stage formula is adopted in the samples of Al-O and Safdar, and the slope of the second stage is assumed to be negative to consider the damage to the tensile zone of UHPC [13, 20]. This type of stress-strain curve is also used in the finite element model calculation in reference [21]. According to the literature conclusion, the results of finite element calculation are in complete accord with the experimental results [27]. In Kazutaka Shirai's sample, only the bottom edge of UHPC is strengthened, and it is assumed that UHPC reaches the design value of tensile strength. This assumption is also considered a two-stage type, and the bottom edge UHPC is in the second stage [28].

In the finite element calculation of Spyridon A. Paschalis's sample, a multistage stress-strain curve is adopted. The stress in the ascending and descending sections is expressed as a function of strain [24]. In Giovanni Martinola's sample, a multistage mode stress-strain curve is also adopted, with the stress in the ascending part as a function of strain and the stress in the descending part as a function of crack width, as shown in Figure 4(b) [24]. The two modes are essentially the same, except that the first mode converts the crack width into cross-section strain.

Due to the super-high compressive performance of UHPC, the concrete in the compression zone rarely reaches the ultimate compressive strength, so UHPC in the compression zone can be assumed to be elastic.

The tensile strength of UHPC was obtained by a splitting strength test [29] or a flexural test [30], while the compressive strength of UHPC was obtained by cylinder specimens [31] or cubic specimens [32].

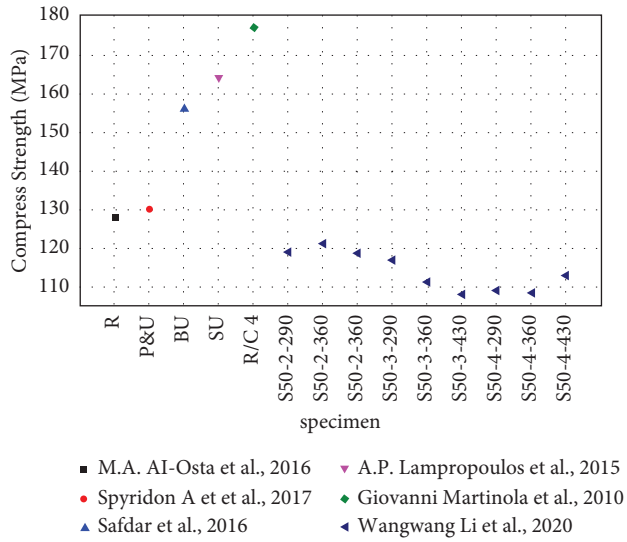

Figure 1: The distribution of UHPC compressive stress.

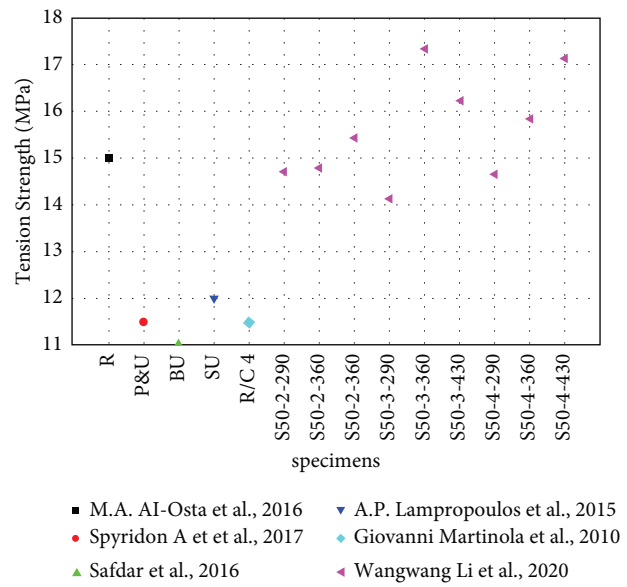

Figure 2: The distribution of UHPC tension stress.

This paper mainly studies the quick calculation method of cracking load and bearing capacity, so a two-stage stress-strain curve is adopted, and the second stage is assumed to be horizontal. The UHPC in the compression zone is also considered to be in the elastic stage, and the stress-strain relationship conforms to Hooke's law.

All the tensile steel reinforcing bars used in the calculation models adopt two-section stress-strain curves, and the second section of most samples is a horizontal straight line, as shown in Figure 5. This stress-strain model is also adopted in this paper.

2.3. Combined Section of Specimens. UHPC is mainly used to improve the ability and durability of reinforced concrete structures, with various combinations. All specimens can be classified into 5 types.

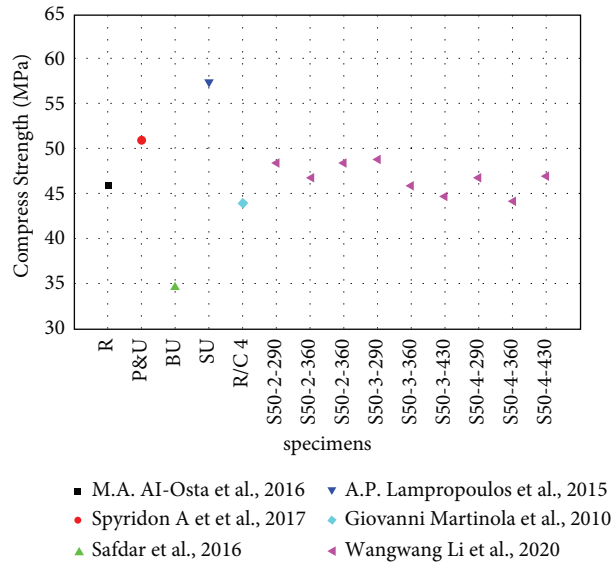

Figure 3: The distribution of NC compressive stress.

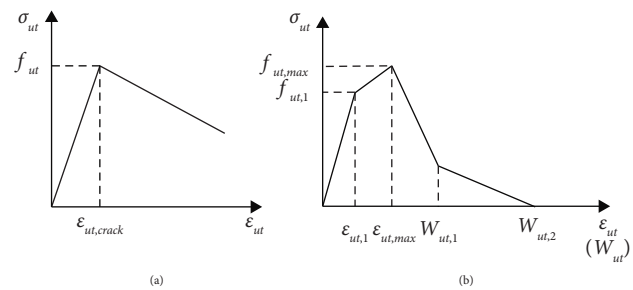

Figure 4: UHPC tensile behavior: (a) Two-stage (b) multistage.

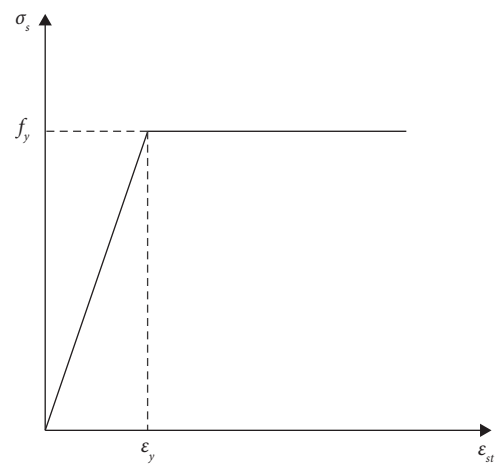

Figure 5: The behavior of steel reinforcing bar in tension.

The bottom edge of the reinforced concrete beam is combined with UHPC, with or without reinforcement in the UHPC layer, as shown in Figure 6(a). This type is the most commonly used combination of UHPC and reinforced concrete, which can significantly improve the bearing capacity and durability of reinforced concrete beams, and the combined effect is obvious. In the case of the UHPC

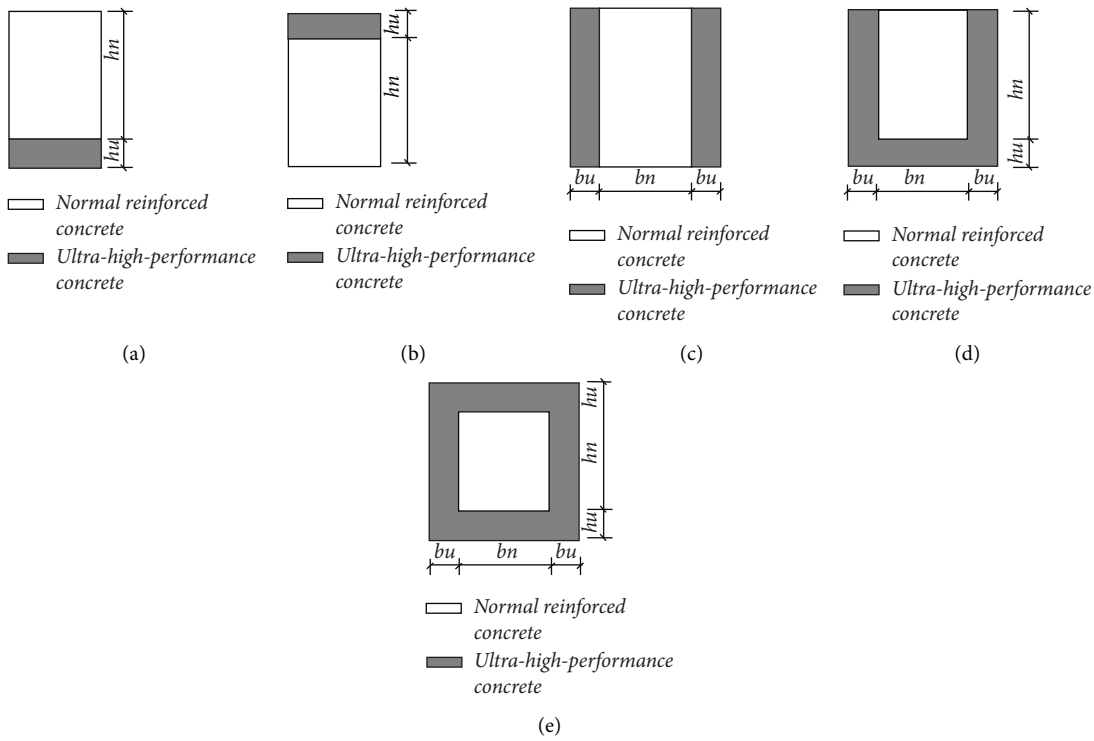

Figure 6: Section details specimens.

reinforced concrete beam, the bottom of the ordinary concrete beam is washed with a high-pressure water gun and then poured with UHPC in most experiments. Besides this way, Tanarslan et al.'s experiment of connecting UHPC laminate to the RC beam by gluing with epoxy resin and mechanical anchoring is also very good.

The top of the reinforced concrete beam is combined with UHPC, generally used to reinforce the original beam when the top edge is cracked or waterproof performance of the beam, as shown in Figure 6(b). As this combination has little influence on the bearing capacity, it will not be discussed in this paper.

Reinforced concrete beams are combined with UHPC on two vertical sides, as shown in Figure 6(c). This form has a good effect on improving shear capacity but a poor effect on improving bending capacity. The combination form can restrain the development of web cracks, is convenient for construction, and can be used to reinforce the webs of box structures.

In jacket combination, reinforced concrete beams are combined with UHPC from the bottom edge and both vertical sides, as shown in Figure 6(d). According to the experimental data, this strengthening method is effective [15, 18].

Full-enclosed reinforcement, UHPC wraps all the original concrete structure, like a hoop, as shown in Figure 6(e). This combination form is less used.

2.4. The Existing Design Model of Flexural Members. The experiments in the literature prove that the junction between UHPC and NC is well connected and can be regarded as the same cross-section [18–21]. So, all calculation models follow the assumption of the plane section even at the junction of UHPC and NC.

2.4.1. The Calculation Mode of Reinforced Concrete. According to design code ACI318 (2008) for RC structures, the simplified rectangular stress diagram is adopted for the compressive stress of ordinary reinforced concrete members, and the tensile stress of concrete is ignored. This calculation model is also adopted in this paper, in which the stress and coefficients are recommended by ACI318 [32].

2.4.2. The Calculation Mode of UHPC in the Tension Zone. In the peak load calculation model, the UHPC stress in the tension zone is distributed as a curve along with the beam height, so the calculation is inconvenient. Scholars simplify the stress curve. The simplified stress distribution along the beam height can be divided into one-stage and two-stage, as shown in Figure 7.

(1) One-stage type

This model assumes that the stress diagram in the tension zone is rectangular, and the UHPC stress value in the tension zone is $\beta\sigma_t$, rectangular height is αh_{ut}. Where β is the stress reduction factor and the height of the tensile zone gives α a reduction factor [33]. This method is easy to calculate, and the acting point of the resultant force is clear. However, the situation that UHPC in the tension zone is still in the elastic stage cannot be considered. The method is

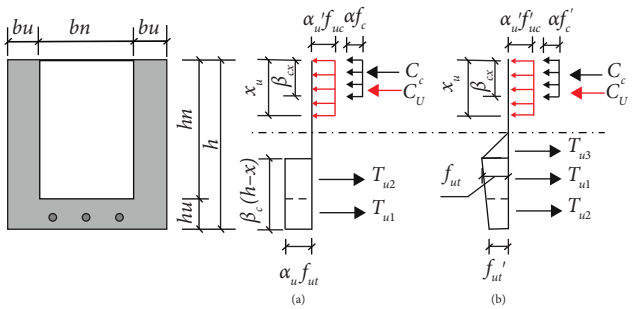

FIGURE 7: The calculation mode of UHPC in the tension zone (a) One-stage type (b) Two-stage type.

suitable for bottom edge reinforcement or combination, and the UHPC layer is thin.

(2) Two-stage type

two-stage calculation mode divides the UHPC layer into elastic and elastic-plastic (with cracks), and considers the constraint of steel reinforcing bars on the cracking of UHPC, without considering the reduction in height and width of the stress diagram. The stress diagram of this method is more accurate, but the calculation process is slightly complicated. Different damage calculation methods will have different stress distributions.

2.5. Prediction Model of the Flexural Capacity of UHPC-Concrete Composite Members. Based on the analysis and research of the above data, to quickly predict the cracking load and peak load of UHPC-NC composite beams, the following calculation model is established. Since the UHPC on the top surface is usually used for waterproofing, the case of UHPC full-enclosure is seldom used in practical projects. So the two types will not be considered in this paper.

Cracking load and peak load are calculated by plane section assumption and equilibrium internal force, as shown in Figure 8. When the cracking load is calculated, UHPC in the tension zone and compression zone is in the elastic stage, and the ordinary concrete in the compression zone is also in the elastic stage. The UHPC at the edge of the tensile zone reaches the tensile strength. The stress of steel reinforcing bars and prestress tendons is calculated by Hooke's law. When the peak load is calculated, the ordinary concrete in compression was represented using the Whitney stress block by the ACI Code [33]; the UHCP in compression was also represented by the rectangular stress block [34]. The UHPC in tension zone adopts a two-stage model, but the plastic UHPC considers two reduction factors. β is the stress reduction factor, and the height of the tensile zone gives α a reduction factor, the values of these two parameters are obtained by trial calculation.

When calculating the cracking load, through the balance of force and moment, we can get the following equations :

$$\sum F = \left(C_s' + C_u + C_c\right) - \left(T_{sn} + T_{u1} + T_{u2} + T_y + T_{su}\right) = 0,$$

$$M = \left(C_c + C_u\right)\left(\frac{2}{3}x\right) + C_s'\left(x - d_s'\right) + T_{sn}\left(d_{sn} - x\right) + T_u\left[\frac{2}{3}\left(h - x\right)\right] + T_y\left(d_y - x\right) + T_{su}\left(d_{su} - x\right). \tag{1}$$

with

$$\begin{aligned} C_s' &= A_{sn}' E_{sn}' \varepsilon_{sn}', \\ C_u &= \frac{1}{2} b_u x \sigma_{uc}', \\ C_c &= \frac{1}{2} b_n x \sigma_c', \\ T_{sn} &= A_{sn} E_{sn} \varepsilon_{sn}, \\ T_{u1} &= \frac{1}{2}\left(2b_u + b_n\right) h_u f_{ut}\left(1 + \frac{\left(h - x - h_u\right)}{\left(h - x\right)}\right), \\ T_{u2} &= b_u \frac{\left(h - x - h_u\right)^2}{\left(h - x\right)} f_{ut}, \\ T_y &= A_y E_y \varepsilon_y, \\ T_{su} &= A_{su} E_{su} \varepsilon_{su}, \end{aligned} \tag{2}$$

where C_s' is resultant force of top reinforcement. A_{sn}' is the area of top edge reinforcement, E_{sn}' is the modulus of top edge reinforcement, ε_{sn}' is the strain of top edge reinforcement;

C_u is UHPC resultant force in compression zone. b_u is width of UHPC one side in compression zone, x is distance from neutral axis to top edge, σ_{uc}' is UHPC stress on the top; C_c is UHPC resultant force in the compression zone. b_n is width of NC in compression zone, σ_c' is NC stress on the top; T_{sn} is the resultant force of steel bars in the bottom NC; it is tensile force. A_{sn} is the area of reinforcement in the bottom NC, E_{sn} is the modulus of reinforcement in the bottom NC, ε_{sn} is the strain of reinforcement in the bottom NC; T_{u1} and T_{u2} is resultant force of UHPC in bottom and sides. h_u height of UHPC in bottom edge, f_{ut} is the cracking stress of UHPC, h is the height of section; T_y is resultant force of prestressed tendon in UHPC, A_y is the area of prestressed tendon in UHPC, E_y is the modulus of prestressed tendon in UHPC, ε_y is the strain of prestressed tendon in UHPC; T_{su} is resultant force of steel bars in bottom UHPC, it's tensile force. A_{su} is the area of reinforcement in the bottom UHPC, E_{su} is the modulus of reinforcement in the bottom UHPC, ε_{su} is the strain of reinforcement in the bottom UHPC; when calculating the peak load, through the balance of force and moment, we can get the following equations:

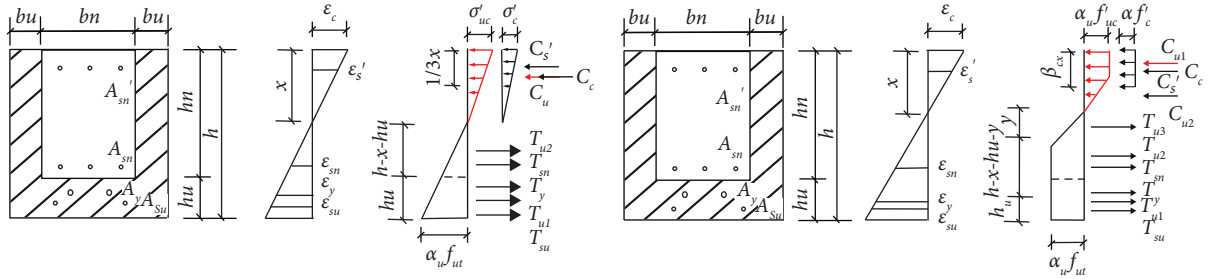

Figure 8: Description of the flexural model. (a) Cracking stain and stress distribution. (b) Stain and stress distribution at failure time.

$$\sum F = \left(C_s' + C_{u1} + C_{u2} + C_c\right) - \left(T_{sn} + T_{u1} + T_{u2} + T_{u3} + T_y + T_{su}\right) = 0, \tag{3a}$$

$$M = \left(1 - \frac{1}{2}\beta_c\right)xC_c + C_s'\left(x - d_s'\right) + C_{u1}\left(x - \frac{1}{2}\beta_{cu}x_u\right) + \frac{2}{3}C_{u2}\left(x - x_u\right) + T_{sn}\left(d_{sn} - x\right) + \frac{2}{3}T_{u3} + T_{u2}\left[y + \frac{1}{2}\left(h - x - h_u - y\right)\right] + T_{u3}\left(h - x - \frac{1}{2}h_u\right) + T_y\left(d_y - x\right) + T_{su}\left(d_{su} - x\right). \tag{3b}$$

with

$$\begin{aligned} C_s' &= A_{sn}'E_{sn}'\varepsilon_{sn}', \\ C_{u1} &= 2b_u\beta_u x_u\alpha_u f_{uc}', \\ C_{u2} &= b_u\left(x - x_u\right)\alpha_u' f_{uc}', \\ C_c &= b_n\beta_c x\alpha f_c', \\ T_{sn} &= A_{sn}f_{sn}, \\ T_{u1} &= \left(2b_u + b_n\right)\beta_u h_u\alpha_u f_{ut}, \\ T_{u2} &= 2b_u\beta_u\left(h - x - h_u - y\right)\alpha_u f_{ut}, \\ T_{u3} &= b_u y\alpha_u f_{ut}, \\ T_y &= A_y f_y, \\ T_{su} &= A_{su}f_{su}, \end{aligned} \tag{4}$$

Where α_u is the stress reduction coefficient of UHPC, β_u is a factor relating the depth of the equivalent rectangular compressive stress block to the depth of the neutral axis of UHPC. Through data trial calculation, $\alpha_u = 0.75, \beta_u = 0.565$. α_c is stress reduction coefficient of NC in compression zone, β_c is factor relating depth of equivalent rectangular compressive stress block to the depth of neutral axis of NC in the compression zone. According to the ACI code [32], $\alpha_c = 1, \beta_c = 0.85 - 0.05f_c' - 28/7f_c' > 28MPa$. y is the height of UHPC in elastic.

Whether cracking load or peak load, the influence of UHPC in the elastic state on axial force and bending moment is considered. In the calculation of cracking load, the upper and lower edge reinforcement and prestress tendons are calculated by Hooke's law; in the calculation of peak load, it is considered that all steel reinforcement bars in the tensile zone have reached the failure stress. However, if the UHPC has poor deformation capacity, the steel bar will not reach the yield stress. So when equations (3a) and 3b are used, the ultimate deformation of UHPC needs to be large enough and it is recommended to exceed 0.005.

This calculation model applies to all reinforcement forms, no matter whether the section of the ordinary concrete is a rectangle, I-section, or box. This model is also suited for reinforced concrete structures and prestressed reinforced concrete structures.

3. Results

3.1. Calculation Results. The data in the literature [15, 18, 22–26] are substituted into the formula and the calculation results are shown in the Table 1.

The cracking load of type 3 combination is determined by ordinary concrete, and the tensile performance of ordinary concrete is poor so this paper does not calculate the cracking load of type 3, but only the peak load.

It can be seen from Table 1 that no matter which combination form is used, the calculation method in this paper is close to the experimental data.

It can be seen from Figure 9 that the difference between the experimental cracking load and the cracking load calculated in this paper is very small. In references [13, 20, 21], the maximum COV of the cracking load is 11.49. So the calculation of cracking load in this paper is accurate. However, the calculation method in this paper of cracking load cannot distinguish the difference between several connection types of UHPC and NC, such as anchoring, epoxy resin bonding, sandblasting, and pouring. According to the original experimental data, after the accidental factors are excluded, the difference between different connection types is small, which can be calculated by the same calculation formula [20]. In reference [12], there is no steel bar in the UHPC layer. In reference [18], steel bars are added to ordinary reinforced concrete and UHPC. In reference [19], the UHPC layer has prestressed tendons. The calculation shows that the cracking load calculated in this paper is very close to the experimental cracking load in references [12, 18, 19], so the model in this paper is suitable for UHPC with and without reinforcement [18, 24, 25].

Table 1: The experimental data and calculated data of UHPC-NC are reported in the literature.

Ref	Specimen name	UHPC			TSSM	fc'	NR		UR		PR		RM	Cracking load				Peak load			
		f_{uc} (Mpa)	f_{ut} (Mpa)	E_u (Gpa)			Area	fsn	Area	fsu	Area	fy		EXP	OR	CAL	COV	EXP	OR	CAL	COV
[18]	R-S-1	128	15	46.0	Two	54	157	680	—		—		1	9.49	—	12.94	—	23.30	24.60	24.99	3.64
	R-S-2												3	11.79				29.30	26.50	28.62	5.19
	R-S-3												4	25.88		26.38		37.90	35.70	41.18	7.21
	R-E-1												1	13.51		12.94		21.60	24.60	24.99	7.82
	R-E-2												3	12.65				27.30	26.50	28.62	3.89
	R-E-3												4	27.31		26.38		37.10	35.70	41.18	7.50
[24]	P1	130	11.5	51.0	Multi	30	226	500	157	500	—		1	—	—	—	—	55.20	51.90	53.45	2.54
	P2												1					54.00			
	U1												1					54.60	58.80	55.09	3.62
	U2												1					56.30			
	UactB1												1					102.10	102.10	106.84	1.98
	UB2												1					105.40			
[22]	BU-20	156	11	34.6	Multi	29.7	402	546	—		—		2	35.00	33.67	—	—	142.20	135.97		
	BU-40												2	38.50	34.67	—	—	148.20	136.00	—	—
	BU-60												2	39.70	34.83	—	—	137.00	136.00		
	BL-20												1	70.50	82.56	66.14	11.64	118.90	140.31	141.71	9.57
	BI-40												1	84.25	87.99	88.39	2.63	145.30	173.32	170.87	9.51
	BI -60												1	88.50	90.62	90.55	2.62	156.30	205.15	198.57	14.20
[15]	SUC	164	12	57.5	—	45.4	226	590	—		—		1					41.00		42.01	1.72
	SUT												2	—	—	—	—	42.00	—	39.11	5.04
	SU3												4					89.00		87.75	1.00
[26]	R/C 4	177	11.5	44.0	Multi	22	0	0	—		—		—	—	—	—	—	410.00	—	408.13	0.32
[25]	S50-2-290	119.12	14.70	48.53	Multi	57.94	—		829	509	278	1353	1	168.90	174.60	178.87	2.87	845.60	751.00	873.00	7.78
	S50-2-360	121.30	14.78	46.85		54.4			1362			1411	1	184.05	190.50	186.50	1.74	867.30	776.80	884.42	6.86
	S50-2-360	118.71	15.43	48.47		63.56						1350	1	198.98	211.80	181.51	7.70	868.80	806.50	867.60	4.20
	S50-3-290	116.97	14.13	48.91		64.09					417	1162	1	228.98	224.10	215.72	3.01	849.30	759.60	844.85	6.18
	S50-3-360	111.29	17.33	45.96		60.52			829	509		1136	1	232.95	231.45	233.68	0.49	873.60	815.80	887.36	4.42
	S50-3-430	108.00	16.22	44.74		51.49						1180	1	251.40	228.30	215.59	7.83	850.90	794.90	864.26	4.40
	S50-4-290	109.04	14.65	46.84		57.67					556	1230	1	287.93	251.63	244.30	8.94	790.00	676.90	730.24	7.73
	S50-4-360	108.53	15.84	44.22		59.16			201			1210	1	285.45	249.08	241.78	9.04	777.40	686.70	800.01	7.95
	S50-4-430	112.96	17.13	46.98		60.97						1230	1	287.63	265.28	271.20	4.22	787.80	738.50	833.40	6.03

Note: 1, TSSM denotes the tensile stress-strain model; NR, denotes the reinforcement in normal concrete; UR, denotes the reinforcement in UHPC; PR denotes the adding prestress tendons in UHPC; RM denotes the reinforcement mode; EXP denotes experimental result; OR denotes calculation result of original literature; CAL denotes calculation result in this paper.2. The cracking load in reference [13] is *P* and the unit is kN, but the peak load is *M* and the unit is kN·m. To avoid misunderstanding, *P* is converted into *M* according to the experimental structure, and the units are kN·m.

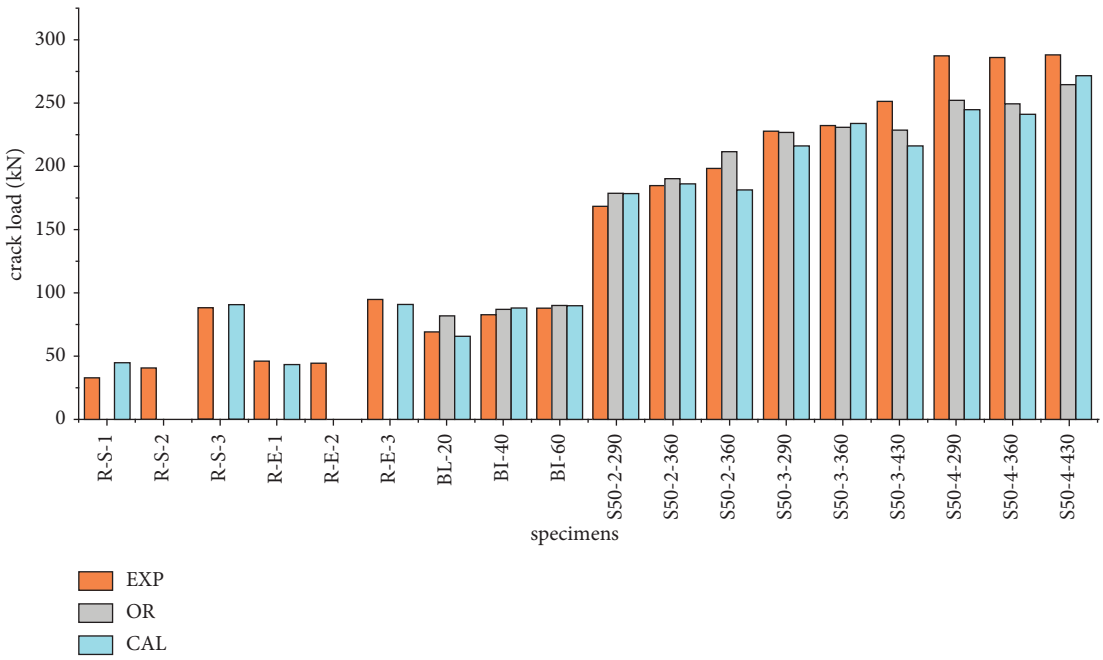

Figure 9: Comparison between the experimental value and the calculated value of cracking load.

It can be seen from Figure 10 that all the peak loads calculated in this paper are close to the experimental values, the maximum COV of the peak load is 14.2. All of the other COVs of the peak load are less than 10; most of the COV are less than 5. Some of the calculation results are closer to the experimental data than the original calculation models. Especially in the calculation of reference [19], there is a big gap between the original calculation results and the experimental values, but the calculation results in this paper are very close to the experimental values. Therefore, this model can calculate the peak load more accurately than other calculation models.

3.2. Analyze the Correlation between Model and Sample. Figure 11 plots the ratio of analysis results to experimental results, including cracking load and peak load, most of which are vertically concentrated between 0.9 and 1.2. Figure 12 plots the measured cracking load versus the corresponding literature cracking load and the current calculated cracking load. The average of M_C(calculation)/M_C(experiment) in this paper is 0.98, with a standard deviation of 0.122. Figure 13 plots the measured peak loads versus the originally calculated peak load and the current calculated peak load. The average of M_p(calculation)/M_p(experiment) in this paper is 1.04, with a standard deviation of 0.08.

Through the comparison of experimental data and calculation results, the calculation results of this model are related to the cracking load and peak load results of all test specimens. The COV of the maximum cracking load is 11.64%, and the maximum creaking load is 14.2; all of them are in the first kind of reinforcement samples in reference [22]. The maximum COV of the cracking load is the BL-20 specimen, in which the UHPC layer is 20 cm; and the maximum COV of peak load is BL-60, in which the UHPC layer is 60 cm.

There is little difference between the calculated results of this model and the experimental results of many projects, and the coefficient of variation is also small. This shows that the calculation model and experimental data adopted in this paper have good applicability. From the data analysis, except for some data, the model adopted in this paper is closer to the experimental value than the original calculation model, especially the peak load in reference [25].

4. Analysis and Discussion

In this study, it can be seen from the abovementioned calculation that the cracking load and peak load of the UHPC-NC beam are affected by many factors. For example, UHPC tensile and compression properties, UHPC ultimate strain, reinforcement strength, and reinforcement area, prestress tendons, and so on.

4.1. UHPC Tensile and Compression Properties. Generally, the tensile strength and compressive strength of UHPC increase together, and the tensile strength is about 1/10 of the compressive strength. It can be seen from equations. (1a) and 1b that the cracking loads are affected by the performance of UHPC. In combination with types 1 and 4, the cracking load was controlled by UHPC tensile stress. Therefore, the cracking load varies with the performance of UHPC. In combination with type 3, the cracking load is controlled by the NC tensile stress, so the crack resistance is no different from ordinary reinforced concrete. If it is structural reinforcement, the cracking signs of type 1 and type 4 reinforcements will be changed from ordinary reinforced concrete cracking to UHPC cracking, and the

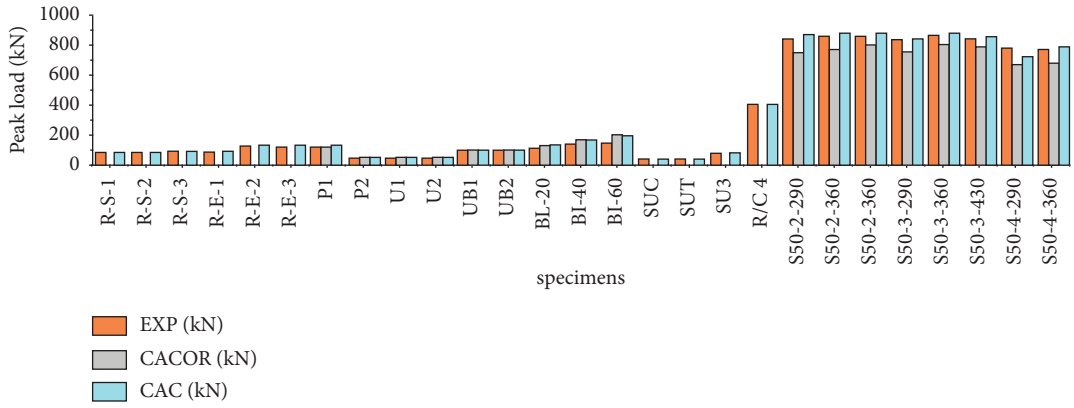

Figure 10: Comparison between the experimental value and calculated value of peak load.

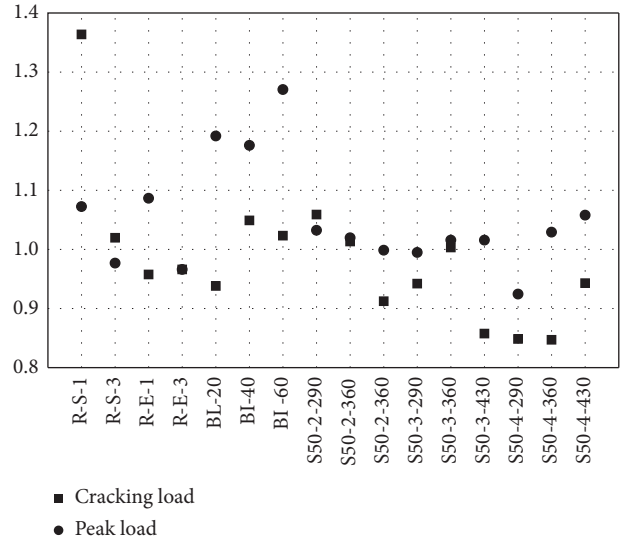

Figure 11: The ratios of the analytical results to the experimental results.

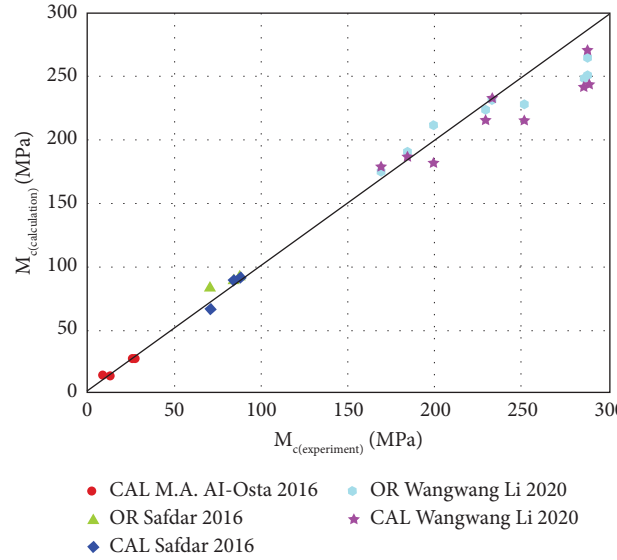

Figure 12: Experimental cracking loads versus the corresponding literate cracking load and the current calculated cracking load.

cracking load will be greatly increased. However, type 3 reinforcement is still marked by the cracking of ordinary reinforced concrete, and the cracking load does not increase too much.

It can be seen from equations (3a) and 3b that UHPC in the tension zone can provide considerable tensile stress, the increase in tensile and compressive strength of UHPC in all reinforcement forms can increase the peak load of the structure.

Based on the experimental sample in reference 12, the compressive strength of UHPC was adjusted, and the tensile strength was assumed to be 1/10 of the compressive strength, and. Figure 14 was obtained. Figure 14 shows the peak load change along with the performance of UHPC in the form of 1.3.4. The peak load of jacket reinforcement increases obviously with UHPC compressive strength, and the bottom edge reinforcement increases most slowly, but the influence of bottom edge reinforcement thickness should also be considered. If the UHPC layer thickens, it can be inferred from equations (3a) and 3b that the slope of type 1 in Figure 14 will become larger.

4.2. Reinforcement Strength and Reinforcement Area. In the design of the UHPC-NC composite beam, if the bottom UHPC layer is thick, steel reinforcing bars can be added; reinforcement cannot be added if the UHPC layer is thin. The strength and area of steel reinforcing bars have a direct impact on the bending performance, whether in the UHPC layer or NC layer. Normally, the steel reinforcing bars in the UHPC layer are far from the neutral axis and deform together with the UHPC. The strength and area have a great influence on the bending performance of the structure. The reinforcement in the UHPC layer is best made of high-strength reinforcement, which matches the good deformation capacity of UHPC. In reference 18, it can be seen that the combination form of adding steel reinforcing bars is 89.6% higher than the original peak load of ordinary reinforced concrete beams, and the combination form of the UHPC layer without steel reinforcing bars is 1.3% higher than that of ordinary reinforced concrete beams. Therefore, if the purpose of combination or reinforcement is to improve peak load, the UHPC layer needs sufficient thickness

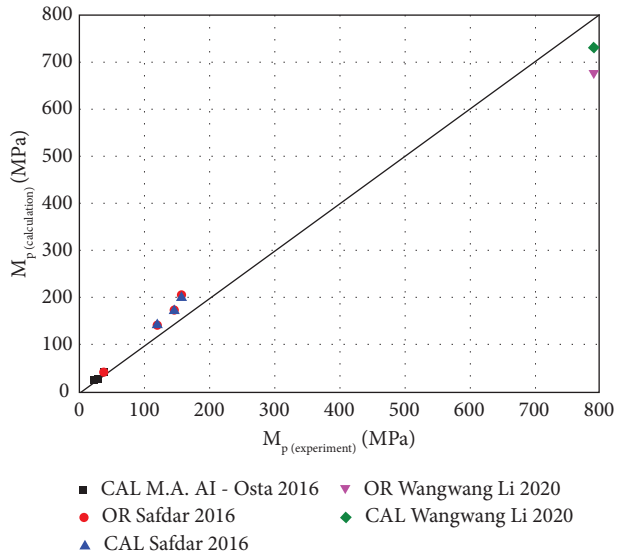

Figure 13: Experimental peak loads versus the corresponding literature sure peak load and the current calculated peak load.

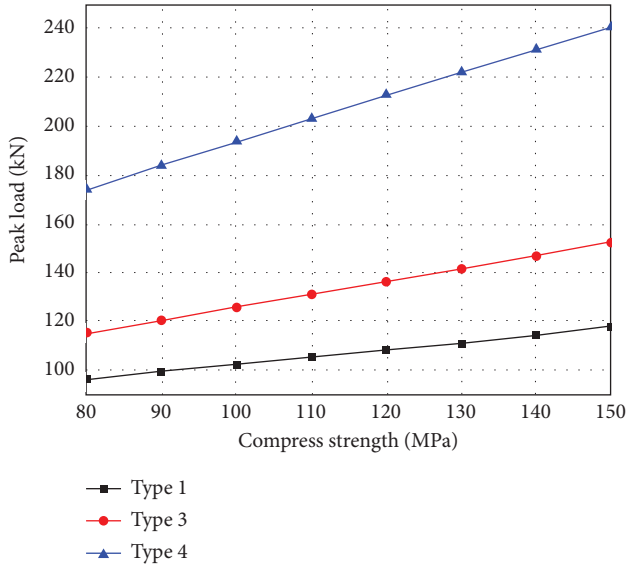

Figure 14: The peak load change with the compressive strength of UHPC.

and high-strength steel reinforcing bars. It is necessary to prevent the super-reinforced beam from crushing the concrete at the top edge when adding steel reinforcing bars and prestressing tendons.

4.3. Prestress Tendons. If UHPC is used to reinforce ordinary concrete, and the prestress tendons are located in ordinary concrete, it is necessary to comply with the specification of ordinary prestressed concrete; if it is the UHPC-NC composite beam, prestress tendons are a better choice in the UHPC layer, which ensures the deformation coordination between UHPC and high-strength prestress tendons and increases cracking load and peak load. So this paper only considers the prestress effect of the UHPC layer.

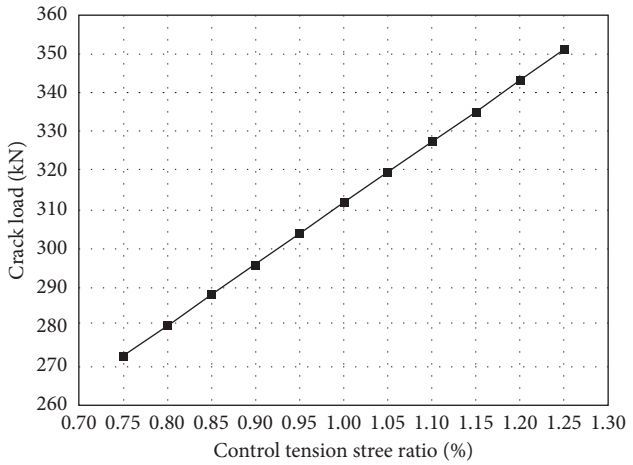

Figure 15: The cracking load change with prestressing ratio.

The width of structural cracks and the structural damage can be reduced by applying prestress, and the bearing capacity of the structure can also be improved. Using a sample in reference [25], adjust the calculation of tension stress controlled by prestressing and get Figure 15. It shows the change of structural cracking load when a different percentage of controlled tensile stress is applied. With the increase of control tension stress of prestress tendons, the cracking load on the structure increases linearly.

5. Conclusions

In this study, a mechanical calculation model for predicting the performance of UHPC flexural members is established and verified. The experimental data of 31 specimens proves that the model is suitable for predicting the cracking load and peak load of UHPC-NC composite beams. The results show that the flexural performance of composite beams can be improved by increasing the strength of UHPC, the area and strength of steel reinforcing bars, and the area and strength of prestress tendons.

(1) In the calculation of cracking load, UHPC is assumed to be elastic, and the stress is distributed in a triangle. In calculating peak load, UHPC is divided into plasticity and elasticity. The elastic part is calculated according to the actual stress distribution; for the plastic part, the calculated height reduction factor β and plastic stress reduction factor α are introduced, and their values are 0.565 and 0.75, respectively, through trial calculation. The calculated results are in good agreement with the data of references.

(2) In the calculation of cracking load, both ordinary steel bars and prestressed tendons are elastic, and the plane section assumption and Hooke's law are used to calculate the stress. In the calculation of peak load, both ordinary steel bars and prestressed tendons are plastic, and the failure load of steel bars is substituted instead of the yield load.

(3) This model is used to calculate three combination types: bottom edge, two vertical sides, and jacket

combination. If it's necessary, it can also be extended to top combination and all-inclusive combination calculations. In this paper, ordinary reinforcement in the NC layer, ordinary reinforcement in the UHPC layer, and prestress tendons in the UHPC layer are also considered. The parameters are considered in detail and have strong applicability. Therefore, the calculation model in this paper has strong applicability and can be applied to various combinations of UHPC-NC beams.

(4) The parameters affecting cracking load and peak load are studied in the paper. The effects of UHPC performance on the bottom edge combination, two vertical combinations, and jacket combination are analyzed. The influence of strength and area of steel bars and prestress tendons is analyzed and calculated. Based on the sample in Ref. [19], the influence of prestress tendons on controlling tensile stress is analyzed. With the increase in the controlled tensile stress of prestress tendons, the cracking load will increase. The model does not consider the different connection modes between UHPC and ordinary concrete. In future research tasks, the influence of these factors will be considered.

Data Availability

The data are available from the corresponding author upon reasonable request.

Conflicts of Interest

The authors declare that they have no conflicts of interest.

Authors' Contributions

Yanru Chen did data collection and developed the methodology; Wei Mao and Yanru Chen wrote the original draft and also reviewed and edited the manuscript; Wei Mao performed supervision. All authors have read and agreed to the published version of the manuscript.

References

[1] P. Richard and M. Cheyrezy, "Composition of reactive powder concretes," *Cement and Concrete Research*, vol. 25, no. 7, pp. 1501–1511, 1995.

[2] B. A. Graybeal and F. Baby, "Development of direct tension test method for ultra-high- performance fiber-reinforced concrete," *Materials*, vol. 110, pp. 177–186, 2013.

[3] D. Y. Yoo and N. Banthia, "Mechanical properties of ultra-high-performance fiber-reinforced concrete: a review," *Cement and Concrete Composites*, vol. 73, pp. 267–280, 2016.

[4] B. A. Graybeal and F. Baby, *Tension Testing of Ultra-high Performance Concrete*, US. Department of Transportation, Washington, DC, USA, 2019.

[5] K. Wille, S. El-Tawil, and A. E. Naaman, "Properties of strain hardening ultra high performance fiber reinforced concrete (UHP-frc) under direct tensile loading," *Cement and Concrete Composites*, vol. 48, pp. 53–66, 2014.

[6] M. Alkaysi, S. El-Tawil, Z. Liu, and W. Hansen, "Effects of silica powder and cement type on durability of ultra high performance concrete (UHPC)," *Cement and Concrete Composites*, vol. 66, pp. 47–56, 2016.

[7] D. Y. Yoo, N. Banthia, and Y. S. Yoon, "Experimental and numerical study on flexural behavior of ultra-high-performance fiber-reinforced concrete beams with low reinforcement ratios," *Canadian Journal of Civil Engineering*, vol. 44, no. 1, pp. 18–28, 2017.

[8] D. Y. Yoo and Y. S. Yoon, "A review on structural behavior, design, and application of ultra-high-performance fiber-reinforced concrete," *International Journal of Concrete Structures and Materials*, vol. 10, no. 2, pp. 125–142, 2016.

[9] W. Fan, D. Shen, T. Yang, and X. Shao, "Experimental and numerical study on low-velocity lateral impact behaviors of RC, UHPFRC and UHPFRC-strengthened columns," *Engineering Structures*, vol. 191, 2019.

[10] D. Y. Yoo and N. Banthia, "Mechanical and structural behaviors of ultra-high-performance fiber-reinforced concrete subjected to impact and blast," *Construction and Building Materials*, vol. 149, pp. 416–431, 2017.

[11] W. Guo, W. Fan, X. Shao, D. Shen, and B. Chen, "Constitutive model of ultra-high-performance fiber-reinforced concrete for low-velocity impact simulations," *Composite Structures*, vol. 185, pp. 307–326, 2018.

[12] W. Fan, X. Xu, Z. Zhang, and X. Shao, "Performance and sensitivity analysis of UHPFRC-strengthened bridge columns subjected to vehicle collisions," *Engineering Structures*, vol. 173, 2018.

[13] W. Fan, D. Shen, Z. Zhang, X. Huang, and X. Shao, "A novel UHPFRC-based protective structure for bridge columns against vehicle collisions: experiment, simulation, and optimization," *Engineering Structures*, vol. 207, Article ID 110247, 2020.

[14] R. Xie, W. Fan, Y. Y. He, B. Liu, and X. Shao, "Crushing behavior and protective performance of varying cores in UHPFRC-steel-foam sandwich structures: experiment, optimal selection and application," *Thin-Walled Structures*, vol. 172, 2022.

[15] A. P. Lampropoulos, S. A. Paschalis, O. T. Tsioulou, and S. E. Dritsos, "Strengthening of reinforced concrete beams using ultra high performance fibre reinforced concrete (UHPFRC)," *Engineering Structures*, vol. 106, pp. 370–384, 2016.

[16] M. Bastien-Masse and E. Brühwiler, "Contribution of R-UHPFRC strengthening layers to the shear resistance of RC elements," *Structural Engineering International*, vol. 26, no. 4, pp. 365–374, 2016.

[17] M. B. Masse, E. Brühwiler, and T. Makita, *Analytical Modelling of R-UHPFRC - RC Composite Members Subjected to Combined Bending and Shear*, Infoscience EPFL Scientific Publication, Lausanne, Switzerland, 2013.

[18] M. Al-Osta, M. N. Isa, M. H. Baluch, and M. K. Rahman, "Flexural behavior of reinforced concrete beams strengthened with ultra-high performance fiber reinforced concrete," *Construction and Building Materials*, vol. 134, pp. 279–296, 2017.

[19] Q. Sun and C. Liu, "Experimental study and calculation method on the flexural resistance of reinforced concrete beam strengthened using high strain-hardening ultra high performance concrete," *Structural Concrete*, vol. 22, no. 3, pp. 1741–1759, 2021.

[20] H. M. Tanarslan, N. Alver, R. Jahangiri, Ç. Yalçınkaya, and H. Yazici, "Flexural strengthening of RC beams using

UHPFRC laminates: bonding techniques and rebar addition," *Construction and Building Materials*, vol. 155, pp. 45–55, 2017.

[21] L. Hussein and L. Amleh, "Structural behavior of ultra-high performance fiber reinforced concrete-normal strength concrete or high strength concrete composite members," *Construction and Building Materials*, vol. 93, pp. 1105–1116, 2015.

[22] M. Safdar, T. Matsumoto, and K. Kakuma, "Flexural behavior of reinforced concrete beams repaired with ultra-high performance fiber reinforced concrete (UHPFRC)," *Composite Structures*, vol. 157, pp. 448–460, 2016.

[23] H. Yin, W. Teo, and K. Shirai, "Experimental investigation on the behaviour of reinforced concrete slabs strengthened with ultra-high performance concrete," *Construction and Building Materials*, vol. 155, pp. 463–474, 2017.

[24] S. A. Paschalis, A. P. Lampropoulos, and O. T. Tsioulou, "Experimental and numerical study of the performance of ultra high performance fiber reinforced concrete for the flexural strengthening of full scale reinforced concrete members," *Construction and Building Materials*, vol. 186, 2018.

[25] W. Li, W. Ji, M. An, L. Zhu, and J. Wang, "Flexural performance of composite prestressed UHPC-NC T-girders," *Journal of Bridge Engineering*, vol. 25, no. 9, Article ID 04020064, 2020.

[26] G. Martinola, A. Meda, G. A. Plizzari, and Z. Rinaldi, "Strengthening and repair of RC beams with fiber reinforced concrete," *Cement and Concrete Composites*, vol. 32, no. 9, pp. 731–739, 2010.

[27] H. Yin, K. Shirai, and W. Teo, "Finite element modelling to predict the flexural behaviour of ultra-high performance concrete members," *Engineering Structures*, vol. 183, 2019.

[28] K. Shirai, H. Yin, and W. Teo, "Flexural capacity prediction of composite RC members strengthened with UHPC based on existing design models," *Structures*, vol. 23, pp. 44–55, 2020.

[29] C. C. Astm, *Standard Test Method for Flexural Performance of Fiber-Reinforced Concrete (Using Beam with Third-Point Loading)*, ASTM International, West Conshohocken, PA, USA, 2012.

[30] Z. Raheem, *Standard Test Method for Compressive Strength of Cylindrical Concrete Specimens 1*, ASTM International, West Conshohocken, PA, USA, 2019.

[31] A. International, "C109-05," *Standard Test Method for Compressive Strength of Hydraulic Cement Mortars*, ASTM International, West Conshohocken, PA, USA, 2005.

[32] ACI Committee 318, *Building code requirements for structural concrete (ACI 318) and commentary*, American Concrete Institute, 2008.

[33] "Anon design considerations for steel fiber reinforced concrete," *Aci Structural Journal*, 1988.

[34] H. C. Mertol, S. H. Rizkalla, P. Zia, and A. Mirmiran, "Characteristics of compressive stress distribution in high-strength concrete," *ACI Structural Journal*, vol. 105, pp. 626–633, 2008.